EurJIC European Journal of Inorganic Chemistry
ChemPubSoc Europe
FULL PAPER

DOI:10.1002/ejic.201402080

Oxidative Addition of Rhodium Complexes Containing a Dithioimidodiphosphinate Ligand: Facile Reductive Elimination of Methyl Iodide from a Tetranuclear Rhodium Sulfido Cluster

Wai-Man Cheung,*[a] Wai-Hang Chiu,[a] Herman H. Y. Sung,[a] Ian D. Williams,[a] and Wa-Hung Leung*[a]

Keywords: Cluster compounds / Rhodium / S ligands / Reduction / Oxidation

Rhodium complexes containing the dithioimidodiphosphinate ligand $[N(iPr_2PS)_2]^-$ have been synthesized and their oxidative addition of methyl iodide investigated. Treatment of $[Rh(PPh_3)_3Cl]$ with $K[N(iPr_2PS)_2]$ afforded $[Rh\{N(iPr_2PS)_2\}(PPh_3)_2]$ (**1**). Recrystallization of **1** from hexane in the presence of adventitious oxygen yielded the peroxo complex $[Rh\{N(iPr_2PS)_2\}(PPh_3)_2(\eta^2\text{-}O_2)]$ (**2**). Oxidative addition of methyl iodide to **1** gave $[Rh(Me)(I)\{N(iPr_2PS)_2\}(PPh_3)_2]$ (**3**), which reacted with $K[N(iPr_2PS)_2]$ to afford $[Rh(Me)\{N(iPr_2PS)_2\}_2]$ (**4**). Treatment of $K[N(iPr_2PS)_2]$ with $[Rh(coe)_2Cl]_2$ (coe = cyclooctene) yielded the tetranuclear sulfido cluster $[Rh_4(\mu_3\text{-}S)_2\{iPr_2PNP(S)iPr_2\}_2\{N(iPr_2PS)_2\}_2]$ (**5**) containing two four-coordinate Rh^I and two five-coordinate Rh^{III} centers. Oxidative addition of methyl iodide to **5** gave the monomethyl compound $[Rh_4(\mu_3\text{-}S)_2(Me)(\mu\text{-}I)\{iPr_2PNP(S)iPr_2\}_2\{N(iPr_2PS)_2\}_2]$ (**6**). In benzene solution, **6** underwent spontaneous reductive elimination of methyl iodide to give **5**. The crystal structures of complexes **2**–**6** have been determined.

Introduction

Transition-metal complexes in sulfur-rich ligand environments are of interest because they are related to the active sites of metalloenzymes[1] and heterogeneous catalysts.[2] Of interest are sulfides of noble metals such as Ru, Os, Rh, and Ir, which are known to be highly active in hydrodesulfurization processes.[3] To gain an insight into the mechanisms of metal sulfide based catalysis, we set out to synthesize metal complexes with sulfur-donor ligands and to explore their organometallic chemistry.

The bidentate dithioimidodiphosphinate ligands $[N(R_2PS)_2]^-$ (R = alkyl, aryl, alkoxy, aryloxy; Scheme 1), which have been recognized as inorganic analogues of acetylacetonate, can bind to main group and transition metals with high electronic and geometric flexibility.[4,5] Previously, we found that Ru and Os complexes with $[N(R_2PS)_2]^-$ (R = Ph, *i*Pr) ligands display rich organometallic and catalytic chemistry. For example, *trans*-$[Os\{N(R_2PS)_2\}_2(OMe)_2]$ can catalyze the aerobic oxidation of PPh_3,[6] whereas Ru carbene complexes with $[N(R_2PS)_2]^-$ are active catalysts for alkene metathesis.[7] As part of our continuing efforts to develop new catalytic processes with metal sulfur complexes, we sought to synthesize Rh dithioimidodiphosphinate complexes and explore their catalytic activity. Our interest in Rh/S systems was stimulated by a report that Rh^{III} thiolate complexes are capable of catalyzing the hydrogenation of imines by heterolytic cleavage of H_2.[8]

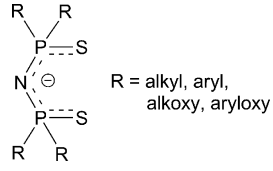

Scheme 1. Structure of $[N(R_2PS)_2]^-$.

Although coordination compounds of $[N(iPr_2PS)_2]^-$, for example, $[M\{N(iPr_2PS)_2\}_2]$ (M = Co, Ni, Zn, Cd),[9,10] are well known, very few Rh complexes with $[N(iPr_2PS)_2]^-$ have been reported. In contrast, Rh complexes containing $[N(Ph_2PS)_2]^-$, for example, $[Rh\{N(Ph_2PS)_2\}(cod)]$ (cod = 1,5-cyclooctadiene)[11] and $[Rh(\eta^5\text{-}C_5Me_5)\{N(Ph_2PS)_2\}X]$ (X^- = Cl^-, tosylate, SCN^-),[12] are well documented. $[Rh\{N(iPr_2PS)_2\}(cod)]$ was recently synthesized from $K[N(iPr_2PS)_2]$ and $[Rh(cod)_2Cl]_2$, but this compound was found to be inactive towards the hydroformylation of styrene.[13a] In this paper, we describe the synthesis of Rh complexes bearing $[N(iPr_2PS)_2]^-$ ligands and their oxidative addition of methyl iodide. We found that the reaction of $K[N(iPr_2PS)_2]$ with $[Rh(coe)_2Cl]_2$ (coe = cyclooctene) afforded the tetranuclear $Rh^{III}_2Rh^I_2$ sulfido cluster $[Rh_4(\mu_3\text{-}S)_2\{iPr_2PNP(S)iPr_2\}_2\{N(iPr_2PS)_2\}_2]$, which underwent oxi-

[a] Department of Chemistry, The Hong Kong University of Science and Technology,
Clear Water Bay, Kowloon, Hong Hong
E-mail: cheungwm@ust.hk
chleung@ust.hk
http://www-chem.ust.hk

dative addition of methyl iodide to afford the $Rh^{III}_3Rh^{I}$ methyl complex $[Rh_4(\mu_3\text{-}S)_2(Me)(\mu\text{-}I)\{i Pr_2PNP(S)iPr_2\}_2\{N(iPr_2PS)_2\}_2]$.

Although the oxidative addition of alkyl halides to low-valent organometallic complexes is well documented, there are very few reports of its microscopic reverse, that is, the reductive elimination of alkyl halides. The reductive elimination of aryl halides from Pd^{IV}[14] and Pt^{IV}[15] centers is, however, well known and the reversible reductive elimination of methyl iodide from $[Ir(CO)_2Cl_3Me]^-$ at high temperature has been studied by IR spectroscopy.[16] Frech and Milstein reported that the reaction of $[\{(C_{10}H_5)(CH_2PR_2)_2\}Rh(Me)(I)]$ (R = *t*Bu) with CO led to the reductive elimination of methyl iodide. In contrast, a similar complex containing a less bulky phenyl-substituted PCP ligand reacted with CO to give a Rh^{III}–CO complex, demonstrating that steric effects are important for the ligand-induced C–I reductive elimination of Rh(PCP) complexes.[17] In this paper we report the facile reductive elimination of methyl iodide from $[Rh_4(\mu_3\text{-}S)_2(Me)(\mu\text{-}I)\{iPr_2PNP(S)iPr_2\}_2\{N(iPr_2PS)_2\}_2]$ in the absence of an added ligand.

Results and Discussion

Phosphine Complexes

Treatment of $[Rh(PPh_3)_3Cl]$ with 1 equiv. of $K[N(iPr_2PS)_2]$ in tetrahydrofuran afforded $[Rh\{N(iPr_2PS)_2\}(PPh_3)_2]$ (**1**; Scheme 2). The $^{31}P\{^1H\}$ NMR spectrum of **1** in $CDCl_3$ displays a doublet of doublets at δ = 46.2 ppm and a doublet at δ = 59.36 ppm that have been assigned to the PPh_3 and $[N(iPr_2PS)_2]^-$ ligands, respectively. Complex **1** is air-sensitive in both the solid state and solution. Upon exposure to air, an orange solution of **1** in $CDCl_3$ gradually turned brown and new resonances at δ = 28.52, 30.99, 61.1, and 64.4 ppm, assignable to a peroxo complex (see below), appeared in the ^{31}P NMR spectrum.

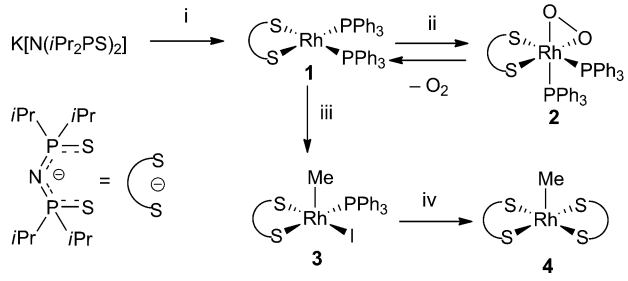

Scheme 2. Synthesis and oxidative addition of Rh phosphine complexes. Reagents: i) $[Rh(PPh_3)_3Cl]$; ii) air; iii) MeI; iv) $K[N(iPr_2PS)_2]$.

An attempt to recrystallize complex **1** from CH_2Cl_2/hexane led to isolation of brown crystals identified as the peroxo complex $[Rh\{N(iPr_2PS)_2\}(PPh_3)_2(\eta^2\text{-}O_2)]$ (**2**). Apparently the peroxo ligand in **2** was derived from adventitious oxygen in the solvent. The O–O stretch in the IR spectrum of **2** was not assigned because it overlaps with an intense ligand band (ca. 884 cm^{-1}). The $^{31}P\{^1H\}$ NMR spectrum of a crystalline sample of **2** in $CDCl_3$ under nitrogen shows four signals at δ = 28.52, 30.99, 61.1, and 64.4 ppm due to **2** along with resonances of **1**. This result shows that the binding of oxygen to **1** is reversible.

The crystal structure of **2** is shown in Figure 1 and its structural parameters are presented in Table 1. The peroxo ligand binds to Rh in a side-on mode with Rh–O and O–O distances of 2.018 (av.) and 1.416(4) Å, respectively, which are similar to those in $[Rh(\eta^2\text{-}O_2)Cl(PPh_3)_3]$ [av. 2.043 and 1.413(9) Å, respectively].[18] The Rh–S (av. 2.426 Å) and Rh–P (av. 2.331 Å) distances are similar to those in **3** [av. 2.385 and 2.2934(11) Å, respectively; see below].

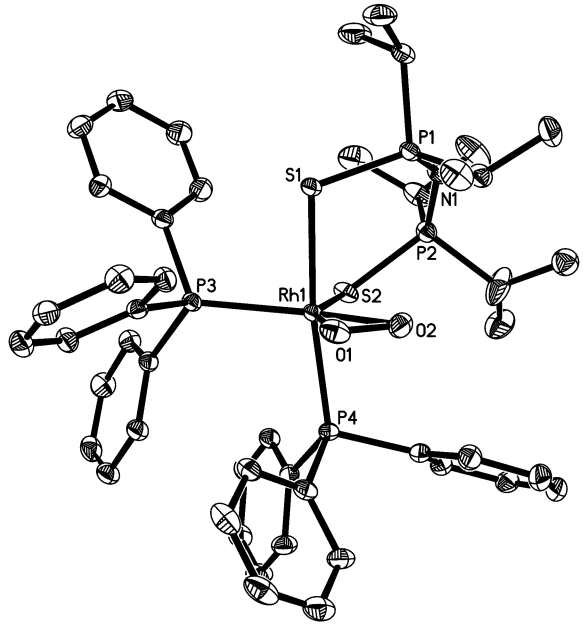

Figure 1. Molecular structure of **2**. Hydrogen atoms have been omitted for clarity. The thermal ellipsoids are drawn at the 30% probability level.

Table 1. Selected bond lengths [Å] and angles [°] for complexes **2**–**4**.

	2	**3**	**4**
Rh–S	2.4199(8)	2.4101(11)	2.3599(5)
	2.4313(10)	2.3603(11)	2.3598(6)
Rh–P	2.3463(9	2.2934(11)	
	2.3157(8)		
Rh–O	2.005(3)		
	2.031(3)		
Rh–C		2.048(4)	2.037(3)
Rh–I		2.6601(6)	
P–S	2.0209(12)	2.0158(15)	2.0305(8)
	2.0327(13)	2.0478(14)	2.0254(8)
P–N	1.576(3)	1.594(4)	1.5998(18)
	1.598(3)	1.585(3)	1.5968(18)
S–Rh–S	93.79(3)	96.76(4)	100.87(2)
P–N–P	136.3(2)	133.2(2)	129.25(12)

Oxidative Addition of Methyl Iodide to 1

Treatment of **1** with excess methyl iodide afforded the five-coordinate Rh^{III} methyl complex $[Rh(Me)(I)\{N(iPr_2PS)_2\}(PPh_3)]$ (**3**). The bis(phosphine) complex was not formed, presumably due to steric effects and a strong

trans influence of the methyl group. The ^{1}H NMR spectrum of the reaction mixture shows a pseudo triplet at δ = 3.12 ppm assignable to the methyl ligand, which indicates that only a single isomer of the product was formed from the oxidative addition. The $^{31}P\{^1H\}$ NMR spectrum displays a doublet at δ = 30.53 ppm assignable to the PPh_3 ligand along with signals from the dithioimidodiphosphinate at δ = 59.51 and 64.9 ppm. Treatment of **3** with $K[N(iPr_2PS)_2]$ resulted in dissociation of the PPh_3 ligand and formation of the bis-chelated complex $[Rh(Me)\{N(iPr_2PS)_2\}_2]$ (**4**). In the ^{1}H NMR spectrum, the methyl protons of **4** appear as a doublet at δ = 3.05 ppm ($^2J_{RhH}$ = 2.8 Hz). The $^{31}P\{^1H\}$ NMR spectrum of **4** displays a singlet at δ = 62.74 ppm, consistent with its solid-state structure. Complex **4** is air-stable in both the solid state and solution. No reaction was observed when **4** was heated in C_6D_6 at 80 °C for 2 h.

Complexes **3** and **4** were characterized by X-ray crystallography (Figures 2, 3, and Table 1). The geometry around Rh in both complexes is pseudo-square pyramidal with the methyl group at the apical position. The Rh–C distances in **3** and **4** [2.048(4) and 2.037(3) Å] are similar to that in

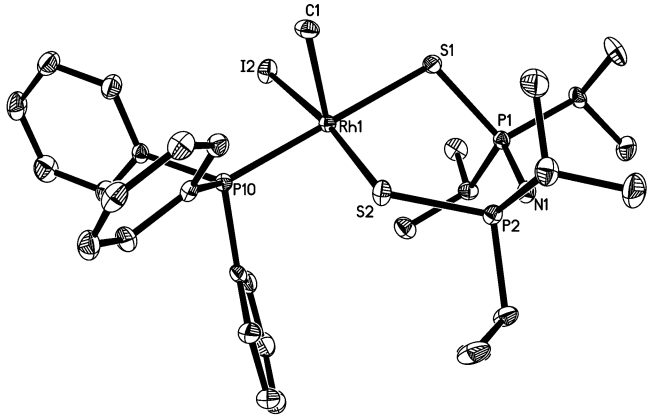

Figure 2. Molecular structure of **3**. Hydrogen atoms have been omitted for clarity. The thermal ellipsoids are drawn at the 30% probability level.

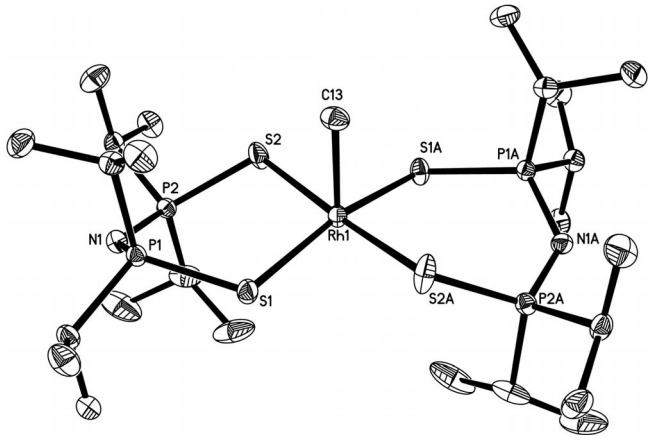

Figure 3. Molecular structure of **4**. Hydrogen atoms have been omitted for clarity. The thermal ellipsoids are drawn at the 30% probability level.

$[RhMe(I)_2(PPh_3)_2]$ [2.081(9) Å].[19,20] In addition, the Rh–S distances in **3** [2.4101(11) and 2.3603(11) Å] and **4** [2.3599(5) and 2.3598(6) Å] compare well with those in **2**.

Tetranuclear Rhodium Sulfido Cluster

Whereas complexes $[Rh\{N(R_2PQ)_2\}(cod)]$ (R = *i*Pr, Q = S;[13a] R = Ph, Q = Se[13b]) were obtained from $K[N(R_2PQ)_2]$ and $[Rh(cod)Cl]_2$, the reaction of $[Rh(coe)_2Cl]_2$ with $K[N(iPr_2PS)_2]$ at room temperature led to the formation of the tetranuclear sulfido cluster $[Rh_4(\mu_3\text{-}S)_2\{iPr_2PNP(S)iPr_2\}_2\{N(iPr_2PS)_2\}_2]$ (**5**) containing two desulfurized $\widehat{PS}$ chelates, $[iPr_2PNP(S)iPr_2]^-$ (Scheme 3). Cluster **5** was also formed as the sole isolable product when the reaction was carried out with different ratios of reactants (1:2–1:4) or solvent (thf). However, heating the reaction mixture at reflux afforded an uncharacterized brown oil that did not crystallize. Note that the mononuclear complex $[Ir\{N(iPr_2PS)_2\}(coe)]$ was obtained from the reaction of the Ir analogue $[Ir(coe)_2Cl]_2$ with $K[N(iPr_2PS)_2]$.[11] Such a difference may be attributed to weaker metal-to-alkene backbonding in the Rh complex, which facilitates the dissociation of the coe ligands and subsequent P–S bond cleavage. Complex **5** is air-sensitive in both the solid state and solution. In addition, it is stable in hexane and benzene solutions under nitrogen, but decomposes readily in CH_2Cl_2. Metal-mediated desulfurization of dithioimidodiphosphinate ligands is well precedented, for example, the reaction of $[Ru_3(CO)_{12}]$ with $HN(Ph_2PS)_2$ in the presence of Me_3NO afforded the sulfido clusters $[Ru_3(\mu_3\text{-}S)_2(CO)_7\{HN(Ph_2P)_2\}]$ and $[Ru_4(\mu_4\text{-}S)_2(\mu\text{-}CO)(CO)_8\{HN(Ph_2P)_2\}]$.[21] The $^{31}P\{^1H\}$ NMR spectrum of **5** shows a doublet at δ = 77.30 ppm (J_{RhP} = 155 Hz) and a singlet at δ = 72.05 ppm, which have been assigned to the Rh-bound phosphino (P4 and P4A) and P=S (P3 and P3A, see Scheme 4) groups of the $[iPr_2PNP(S)iPr_2]^-$ ligands, respectively. In addition, a doublet of doublets at δ = 61.64 ppm (J_{PP} = 24.4, J_{RhP} = 3.9 Hz) and a doublet at δ = 59.12 ppm (J_{PP} = 24.4 Hz) were observed, which have been assigned to the bridging (P1 and P1A) and non-bridging (P2 and P2A) P=S groups of the $[N(iPr_2PS)_2]^-$ ligands, respectively,.

The solid-state structure of **5** featuring a $\{Rh_4S_2\}^{4+}$ core is shown in Figure 4. The geometry around Rh1 is distorted square pyramidal with the phosphino group at the apical position, whereas that around Rh2 is pseudo-square planar (sum of the bond angles: 362.87°). On the basis of the observed coordination geometry, the oxidation states of Rh1 and Rh2 have been tentatively assigned as +3 and +1, respectively, and thus **5** is formulated as a mixed valence $Rh^I_2Rh^{III}_2$ cluster. Consistent with this assignment, the electron-rich Rh2 center can undergo oxidative addition of methyl iodide to give a Rh^{III} methyl species (see below). The Rh1–Rh2/2A separations are quite long [2.9919(6), 3.0086(9), and 3.0760(6) Å], which indicates that there are no or very weak interactions between the Rh centers. The Rh···μ_3-S distances (av. 2.2825 Å) are shorter than those in $[Rh_3(\mu\text{-}Cl)_2(\mu_3\text{-}S)_2(\mu\text{-}S)(PEt_3)_6][PF_6]$ (av. 2.379 Å).[22] The

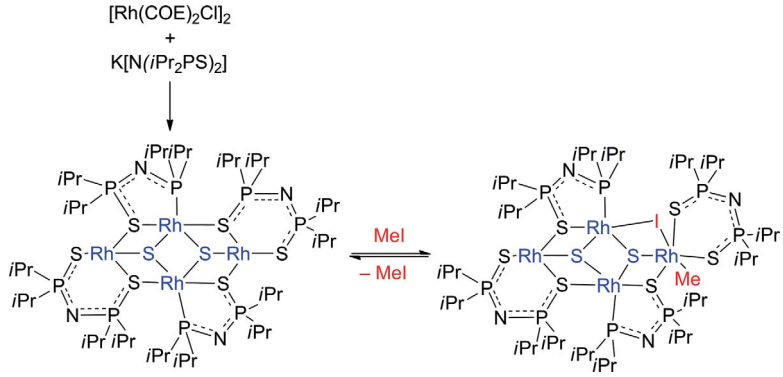

Scheme 3. Reversible oxidative addition of MeI to the Rh_4S_2 cluster **5**.

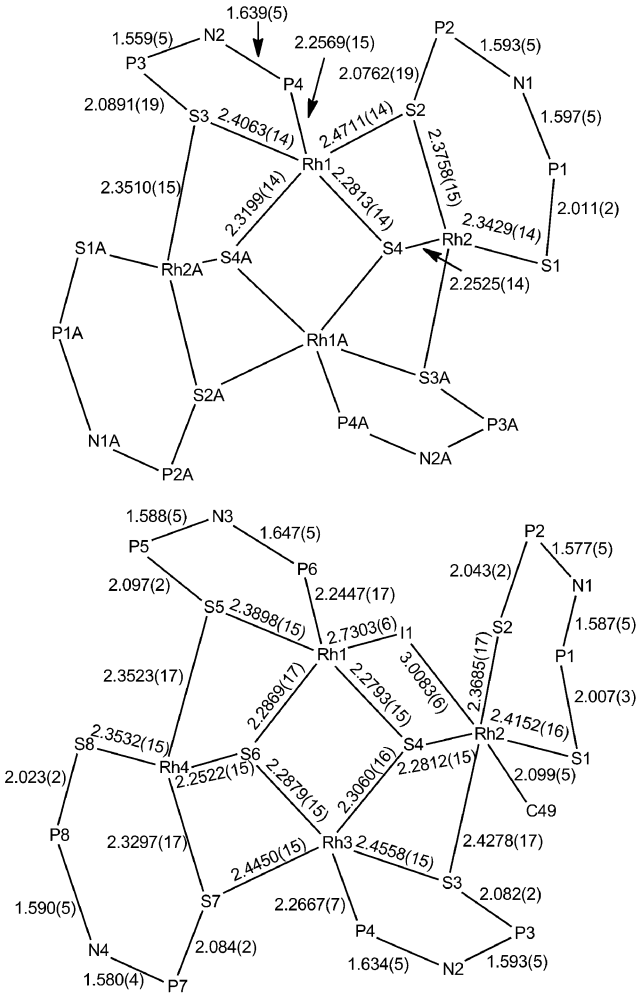

Scheme 4. Selected bond lengths [Å] in **5** and **6**.

two sulfides are located approximately 1.473 Å above the Rh_3 mean plane with Rh···μ_3-S distances of 2.2525(14), 2.2813(14), and 2.3199(14) Å. These distances compare well with those in $[Rh_3(\mu\text{-}Cl)_2(\mu_3\text{-}S)_2(\mu\text{-}S)(PEt_3)_6][PF_6]$ (av. 2.379 Å),[22] $[NMe_4][Rh_3(\mu_3\text{-}S)_2(CO)_6]$ (av. 2.351 Å),[23] and $[(Cp^*Rh)_3(\mu\text{-}Cl)_2(\mu_3\text{-}S)(\mu\text{-}S\textit{i}Pr)][BPh_4]$ (Cp^* = η^5-C_5Me_5; av. 2.368 Å).[24] The $[N(\textit{i}Pr_2PS)_2]^-$ and $[\textit{i}Pr_2PNP(S)\textit{i}Pr_2]^-$ ligands bind to the Rh atoms in a μ:κ_2,κ_1 fashion. The κ_3 binding mode of the $[N(R_2PS)_2]^-$ ligand has been previously found in other systems such as $[Mn_2(CO)_6\{N(Me_2PS)_2\}_2]$.[25] The S–Rh–S bite angle of 106.13(5)° in **5** is considerably larger than that in $[Rh\{N(Ph_2PS)_2\}(cod)]$ [98.48(3)°][9,13a] due to the formation of the Rh–S–Rh bridge. In the Rh–S–P–N–P–S metallacycle, the Rh2···μ-S2 distance [2.3758(15) Å] is longer than that of Rh2–S1 [2.3429(14) Å], whereas the P2···μ-S2 distance [2.0762(19) Å] is longer than the P1–S1 distance [2.011(2) Å].

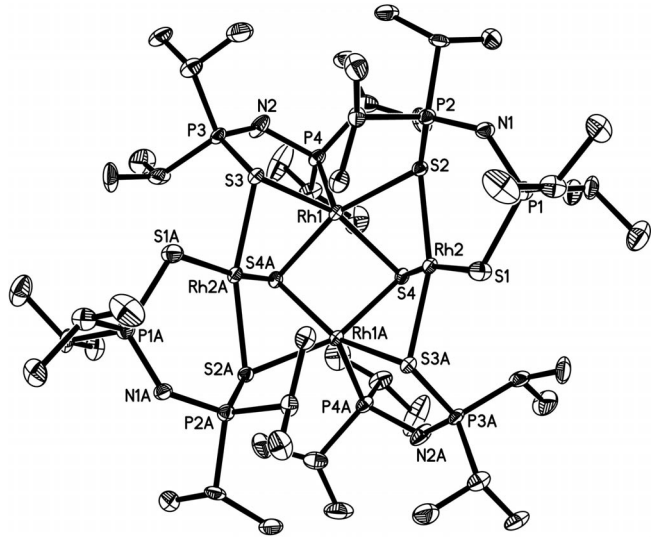

Figure 4. Molecular structure of **5**. Hydrogen atoms have been omitted for clarity. The thermal ellipsoids are drawn at the 30% probability level.

Reversible Oxidative Addition of Methyl Iodide to 5

The oxidative addition of methyl iodide to **5** in C_6D_6 was monitored by $^{31}P\{^1H\}$ NMR spectroscopy (Figure 5). Treatment of **5** with 1 equiv. of methyl iodide resulted in the formation of an approximately 1:1 mixture of **5** and a new species, **6**, which exhibits resonances at δ = 55.93, 57.56, 61.72, 65.62, 71.87, 74.83, 96.91, and 103.85 ppm in the $^{31}P\{^1H\}$ NMR spectrum (Figure 5, b). Complex **5** was converted into **6** almost completely upon addition of excess (≥ 20-fold) methyl iodide to the reaction mixture (Figure 5, c). Recrystallization of **6** from hexane at –10 °C in the pres-

ence of methyl iodide afforded single crystals, which were identified as the monomethyl complex $[Rh_4(\mu_3\text{-}S)_2(Me)(\mu\text{-}I)\{iPr_2PNP(S)iPr_2\}_2\{N(iPr_2PS)_2\}_2]$ by X-ray crystallography. A preliminary study showed that **5** also reacted with other alkyl halides such as benzyl chloride and ethyl iodide. However, these reactions gave hexane-insoluble materials that could not be crystallized. Complex **6** is air-sensitive in both the solid state and solution, and is stable in hexane and benzene, but decomposes readily in more polar solvents such as CH_2Cl_2. In an attempt to prepare a Rh acyl cluster, the reaction of **6** with CO was studied. When a thf solution of **6** was stirred under an atmosphere of CO, the green solution turned reddish brown immediately. The IR spectrum of the crude product displays C–O bands at 1998 and 2064 cm^{-1}, which indicates that it is possibly a Rh carbonyl species. Despite several attempts, we were unable to crystallize the brown carbonylated product.

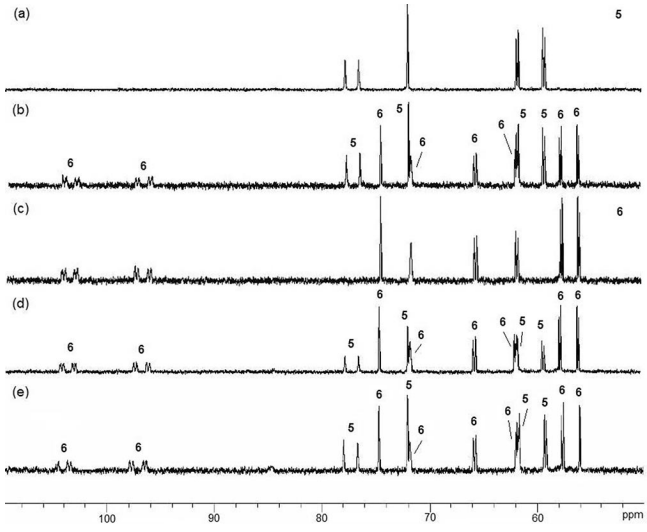

Figure 5. $^{31}P\{^1H\}$ NMR spectra (C_6D_6, 162 MHz, 298 K) of **5** (a), after addition of 1 equiv. of MeI (b), after addition of 20 equiv. of MeI (c), and **6** in C_6D_6 after 20 (d) and 45 min (e).

Dissolution of crystalline **6** in C_6D_6 resulted in the formation an approximately 1:1 mixture of **5** and **6**, according to ^{31}P NMR spectroscopy (Figure 5, e). This indicates that in benzene solution **6** is in equilibrium with **5** and methyl iodide, and that the equilibrium constant is roughly equal to one at room temperature. The reductive elimination of **6** can be completely inhibited by the addition of excess (≥ 20-fold) methyl iodide. Under these condition, only resonances due to **6** were observed in the ^{31}P NMR spectrum. The ^1H NMR spectrum of **6** in C_6D_6/CH_3I (100:1, v/v) shows a doublet at δ = 2.98 ppm assignable to the Rh-bound methyl anion ligand. Despite the presence of excess methyl iodide, there is no evidence for a second oxidative addition of methyl iodide to **5** to give a dimethyl complex, presumably because the oxidation of one Rh center, Rh2, leads to deactivation of the other Rh^I center towards oxidative addition in the cluster.[26] Treatment of **6** with a 20-fold excess of CD_3I in benzene yielded the labeled compound [D_3]**6**, which was characterized by ^2H NMR spectroscopy. This result suggests the oxidative addition of methyl iodide to **5** is truly reversible.

Figure 6 shows the molecular structure of **6** and selected bond lengths in **5** and **6** are listed in Scheme 4 for comparison. The major difference between the structures of **6** and **5** is that, after the oxidative addition, the geometry around Rh2 changes from pseudo-square planar to octahedral with the newly formed Rh–C bond opposite the iodo ligand. In addition, the Rh1–S2 bond in **5** is replaced by the Rh1–I bond. Thus, it is reasonable to assume that the oxidative addition of **5** occurs at Rh2, and **6** can be formulated as a $Rh^IRh^{III}_3$ cluster. The Rh–C distance of 2.099(5) Å is slightly longer than those in **3** and **4**. The iodo ligand bridges Rh1 and Rh2 unsymmetrically with Rh1···μ-I and Rh2···μ-I distances of 2.7303(6) and 3.0083(6) Å, respectively. The Rh2–I bond is rather long, presumably due to the *trans* influence of the opposite methyl group. In addition, the Rh2–S1 and Rh2–S3 bonds in **6** are longer than those in **5**, possibly due to steric effects. The metal–ligand bond lengths and angles of the other Rh centers in **6** are similar to those in **5**.

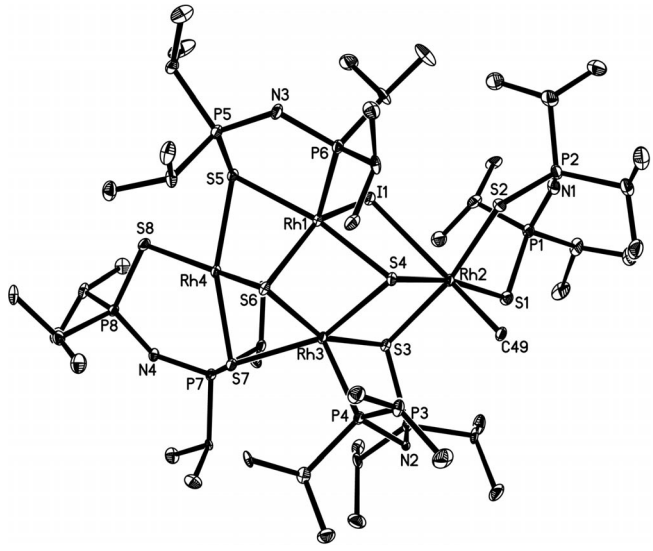

Figure 6. Molecular structure of **6**. Hydrogen atoms have been omitted for clarity. The thermal ellipsoids are drawn at the 30% probability level.

Contrary to the mononuclear analogue **3**, which is stable with respect to reductive elimination, tetranuclear **6** undergoes reversible oxidative addition/reductive elimination with methyl iodide in solution. The ease of reductive elimination of methyl iodide from Rh2 in **6** may be attributed to the cooperative effect of the adjacent Rh1 center, which presumably assists C–I bond formation and Rh1–C bond breaking. In addition, the trivalent Rh1 center makes Rh2 more electron-poor, thereby facilitating the reductive elimination. Such a cooperative effect has been previously observed in the oxidative addition of related dinuclear M^IM^{III} (M = Ir, Rh) systems with alkyl halides.[26] Furthermore, the ability of the sulfur ligands in **6** to stabilize both the +3 and +1 oxidation states of Rh may play a role in the reductive elimination.

The results of previous studies suggested that two pathways are possible for the Rh-centered reductive elimination of methyl iodide: (a) Concerted reductive elimination via a four-center transition state and (b) dissociation of iodide to give a cationic intermediate followed by nucleophilic attack (S_N2 type) on the methyl group (Scheme 5).[17] In this work, we found that the addition of nBu$_4$NI (ca. 50 equiv.) has very little influence on the reductive elimination of **6** in C_6D_6, ruling out pathway b. Therefore we believe that a concerted mechanism involving a four-center transition state (pathway a) is operative in the reductive elimination of **6**. It seems likely that **6** rearranges to the *cis* form, *cis*-**6**, in which the methyl and iodide groups are mutually *cis*, before the reductive elimination takes place. Recently, Feller, Milstein and co-workers reported that polar solvents such as acetone increase the rate of S_N2 reductive elimination of methyl iodide from the Rh(PCP) complexes.[17c] Unfortunately, we were not able to examine the solvent effect on the reductive elimination of **6** because **6** decomposes readily in polar protic/aprotic solvents such as CH_2Cl_2 and acetone.

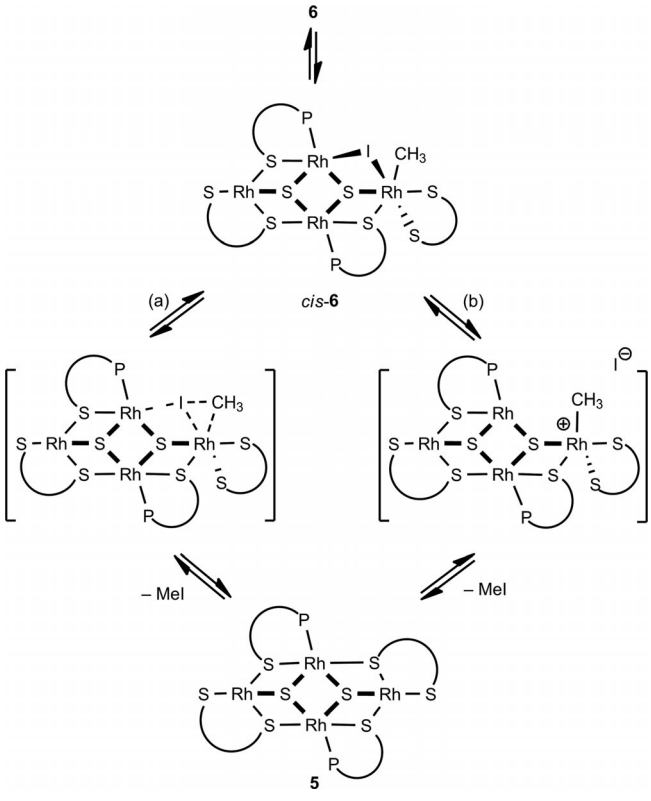

Scheme 5. Proposed reaction pathways for the reductive elimination of methyl iodide from **6**.

Conclusions

We have synthesized and characterized Rh complexes with $[N(iPr_2PS)_2]^-$ ligands and investigated their oxidative addition reactions. The reaction of $[Rh\{N(iPr_2PS)_2\}(PPh_3)_2]$ with oxygen and methyl iodide yielded the peroxo $[Rh\{N(iPr_2PS)_2\}(PPh_3)_2(\eta^2\text{-}O_2)]$ and methyl $[Rh(Me)(I)\{N(iPr_2PS)_2\}(PPh_3)]$ compounds, respectively. Treatment of $[Rh(coe)_2Cl]_2$ with $K[N(iPr_2PS)_2]$ resulted in desulfurization of the imidodiphosphinate ligand and formation of a tetranuclear $Rh^{III}_2Rh^{I}_2$ sulfido cluster, **5**, featuring a Rh_4S_2 core. Complex **5** underwent reversible oxidative addition of methyl iodide to give the $Rh^{III}_3Rh^{I}$ monomethyl cluster **6**. In solution, in the absence of methyl iodide, cluster **6** underwent spontaneous reductive elimination of methyl iodide. The Rh sulfido cluster **5** undergoes facile oxidative addition/reductive elimination, possibly because of the cooperative effect of neighboring Rh centers in the cluster and/or the ability of the sulfur ligands to stabilize both the Rh^{I} and Rh^{III} states. Therefore one may expect electron-rich Rh/S clusters to display interesting organometallic chemistry and are potentially useful in catalytic reactions. A preliminary study showed that **5** can also undergo oxidative addition of silanes such as Et_3SiH. An investigation of the catalytic activity of **5** is underway.

Experimental Section

General: All manipulations were carried out under nitrogen by using standard Schlenk techniques. Solvents were purified, distilled, and degassed prior to use. NMR spectra were recorded with a Bruker AV 400 spectrometer operating at 400 and 162 MHz for ^{1}H and ^{31}P NMR, respectively. Chemical shifts (δ, ppm) are reported with reference to $SiMe_4$ (^{1}H) and H_3PO_4 (^{31}P). IR spectra were recorded with a Perkin–Elmer 16 PC FT-IR spectrophotometer. Mass spectra were recorded with an Applied Bio-system QSTAR mass spectrometer. Elemental analyses were performed by Medac Ltd., Surrey, UK. $K[N(iPr_2PS)_2]$,[27] $[Rh(PPh_3)_3Cl]$[28], and $[Rh(coe)_2Cl]_2$ (coe = cyclooctene)[29] were prepared according to literature methods.

$[Rh\{N(iPr_2PS)_2\}(PPh_3)_2]$ (1): $K[N(iPr_2PS)_2]$ (35 mg, 0.10 mmol, 1 equiv.) was added to a solution of $[Rh(PPh_3)_3Cl]$ (92 mg, 0.10 mmol) in thf (10 mL) and the mixture stirred at room temperature for 2 h, during which the red solution turned orange. The solvent was pumped off and the residue washed with hexane and extracted with CH_2Cl_2/hexane (1:1, v/v). Concentration and cooling to –10 °C afforded an orange crystalline solid, yield 56 mg (60%). ^{1}H NMR (C_6D_6): δ = 1.27 [m, 24 H, $(CH_3)_2CH$], 2.03 [m, 4 H, $(CH_3)_2CH$], 7.03 (m, 18 H, Ph), 7.88 (m, 12 H, Ph) ppm. ^{31}P{^{1}H} NMR (C_6D_6): δ = 46.19 (dd, J = 15, 179 Hz, PPh_3), 59.36 (d, J = 15 Hz, $[N(iPr_2PS)_2]^-$) ppm. $C_{48}H_{58}NP_4RhS_2\cdot0.5CH_2Cl_2$ (939.91): calcd. C 59.30, H 6.05, N 1.43; found C 59.79, H 6.16, N 1.44.

$[Rh\{N(iPr_2PS)_2\}(PPh_3)_2(\eta^2\text{-}O_2)]$ (2): Recrystallization of **1** from a saturated CH_2Cl_2/hexane solution for 1 week afforded red crystals suitable for X-ray diffraction, yield 10 mg (10%). ^{31}P{^{1}H} NMR (C_6D_6): δ = 28.52 (m, PPh_3), 30.99 (m, PPh_3), 61.1 (m, $[N(iPr_2PS)_2]^-$), 64.40 (m, $[N(iPr_2PS)_2]^-$) ppm together with resonances of **1**. $C_{48}H_{58}NO_2P_4RhS_2$ (971.91): calcd. C 59.32, H 6.02, N 1.44; found C 59.60, H 5.91, N 1.25.

$[Rh(Me)(I)\{N(iPr_2PS)_2\}(PPh_3)]$ (3): Methyl iodide (83 µL, 1.33 mmol, 20 equiv.) was added to a solution of complex **1** (62 mg, 0.066 mmol) in thf (10 mL) and the mixture stirred at room temperature overnight. The solvent was removed in vacuo and the residue was washed with hexane and extracted with thf/hexane (1:5,

v/v). Concentration and cooling to –10 °C afforded dark-brown crystals, yield 33 mg (40%). ^{1}H NMR (C_6D_6): δ = 1.08 [m, 24 H, (CH_3)$_2$CH], 1.90 [m, 4 H, (CH_3)$_2$CH], 3.12 (t, J = 3.0 Hz, 3 H, Me), 7.03 (m, 18 H, Ph), 7.88 (m, 12 H, Ph) ppm. ^{31}P{^{1}H} NMR (C_6D_6): δ = 30.53 (d, J = 128 Hz, PPh_3), 59.51 (m, [N(iPr$_2$PS)$_2$]$^-$), 64.94 (m, [N(iPr$_2$PS)$_2$]$^-$) ppm. MS (ESI): m/z = 692 [M – I]$^+$. $C_{31}H_{46}INP_3RhS_2$·0.2C_6H_{14} (819.56): calcd. C 46.22, H 5.88, N 1.67; found C 46.09, H 5.66, N 1.36.

[Rh(Me){N(iPr$_2$PS)$_2$}$_2$] (4): K[N(iPr$_2$PS)$_2$] (12 mg, 0.033 mmol, 1.1 equiv.) was added to a solution of complex **3** (28 mg, 0.030 mmol) in thf (10 mL) and the reaction mixture was stirred at room temperature overnight. The solvent was removed in vacuo and the residue extracted with hexane. Concentration and cooling to –10 °C afforded red crystals, yield 12 mg (47%). ^{1}H NMR (C_6D_6): δ = 1.24 [m, 48 H, (CH_3)$_2$CH], 2.07 [m, 8 H, (CH_3)$_2$CH], 3.05 (d, J = 2.8 Hz, 3 H, CH_3) ppm. ^{31}P{^{1}H} NMR (C_6D_6): δ = 62.74 (s) ppm. $C_{25}H_{59}N_2P_4RhS_4$·0.5C_6H_{14} (742.81): calcd. C 41.90, H 8.60, N 3.62; found C 42.08, H 8.27, N 3.58.

[Rh$_4$(μ_3-S)$_2${iPr$_2$PNP(S)iPr$_2$}$_2${N(iPr$_2$PS)$_2$}$_2$] (5): K[N(iPr$_2$PS)$_2$] (59 mg, 0.17 mmol, 2 equiv.) was added to a suspension of [Rh(coe)$_2$Cl]$_2$ (60 mg, 0.084 mmol) in Et_2O (10 mL), and the reaction mixture was stirred at room temperature for 2 h. The solvent was pumped off and the residue extracted with hexane. Concentration and cooling to –10 °C afforded deep-brown crystals, yield 39 mg (55%). ^{1}H NMR (C_6D_6): δ = 1.15–3.84 (m, 112 H) ppm. ^{31}P{^{1}H} NMR (C_6D_6): δ = 59.12 (d, $^2J_{PP}$ = 24.4 Hz, P2), 61.64 (dd, $^2J_{RhP}$ = 3.9 Hz, $^2J_{PP}$ = 24.4 Hz, P1), 72.05 (s, P3), 77.30 (d, $^1J_{RhP}$ = 155 Hz, P4) ppm (see Scheme 4 for the phosphorus atom-labelling scheme). $C_{48}H_{112}N_4P_8Rh_4S_8$·0.5$C_6H_{14}$ (1661.36): calcd. C 35.94, H 7.04, N 3.29; found C 36.39, H 7.23, N 3.17.

[Rh$_4$(μ_3-S)$_2$(Me)(μ-I){iPr$_2$PNP(S)iPr$_2$}$_2${N(iPr$_2$PS)$_2$}$_2$] (6): Methyl iodide (23 μL, 0.36 mmol, 20 equiv.) was added to a solution of **5** (30 mg, 0.018 mg) in thf/Et_2O (1:1, v/v, 10 mL) and the reaction mixture was stirred at room temperature for 5 min during which the brown solution turned green. The solvent was pumped off and the residue extracted with hexane. Concentration and cooling to –10 °C afforded deep-green crystals. A second crop of **6** was obtained by the addition of 1 drop of methyl iodide to the mother liquor and cooling to –10 °C, yield 22 mg (67%). ^{1}H NMR (C_6D_6/CH_3I, 100:1, v/v): δ = 1.36–3.90 (m, 112 H), 2.98 (d, $^2J_{RhH}$ = 2.5 Hz, 3 H, CH_3) ppm. ^{31}P{^{1}H} NMR (C_6D_6): δ = 55.93 (dd, $^2J_{RhP}$ = 4.5 Hz, $^2J_{PP}$ = 21.0 Hz, P2), 57.56 (dd, $^2J_{RhP}$ = 3.2 Hz, $^2J_{PP}$ = 21.0 Hz, P1), 61.72 (d, $^2J_{PP}$ = 27.5 Hz, P5), 65.62 (d, $^2J_{PP}$ = 27.5 Hz, P3), 71.87 (br. s, P8), 74.83 (s, P7), 96.91 (m, P6), 103.85 (m, P4) ppm. $C_{49}H_{115}IN_4P_8Rh_4S_8$·0.5$C_6H_{14}$ (1803.30): calcd. C 33.83, H 6.67, N 3.03; found C 34.26, H 6.71, N 2.89.

Reaction of 6 with CD_3I: CD_3I (7 μL, 0.11 mmol, 20 equiv.) was added to a solution of **6** (10 mg, 0.0055 mmol) in C_6D_6 (0.5 mL). NMR spectra were recorded after 1 h. ^{2}H NMR (C_6D_6): δ = 2.96 (m, 3 D, CD_3) ppm. ^{31}P{^{1}H} NMR (C_6D_6): δ = 56.05 (d, J = 21.2 Hz), 57.56 (d, J = 21.2 Hz), 61.81 (d, J = 27.5 Hz), 65.75 (d, J = 27.5 Hz), 71.87 (s), 74.70 (s), 97.13 (m), 104.14 (m) ppm.

X-ray Crystallography: Crystal data and experimental details for **2**–**6** are summarized in Table 2. Preliminary examinations and intensity data collection were preformed with a Bruker SMART-APEX 1000 area-detector diffractometer using graphite-monochromated Mo-K_α radiation (λ = 0.70173 Å) (for **3**, **5** and **6**) or Oxford Diffraction (for **2** and **4**). The data were corrected for absorption using the program SADABS[30] (for **3**, **5** and **6**) or CrysAlis RED[31] (for **2** and **4**). Structures were solved by direct methods and refined by full-matrix least-squares on F^2 using the SHELXTL software package.[32] Unless stated otherwise, non-hydrogen atoms were refined with anisotropic displacement parameters. Carbon-bonded hydrogen atoms were included in calculated positions and refined in the riding mode using the SHELXL97 default parameters.

CCDC-974694 (for **3**), -974695 (for **2**), -974696 (for **4**), 974697 (for **5**), and 974698 (for **6**) contain the supplementary crystallography data for this paper. These data can be obtained free of charge from The Cambridge Crystallographic Data Centre via www.ccdc.cam.ac.uk/data_request/cif.

Table 2. Crystallographic data and experimental details for **2**–**6**.

	2	**3**	**4**	**5**	**6**·0.25C_6H_{14}
Empirical formula	$C_{48}H_{65}NO_2P_4RhS_2$	$C_{31}H_{46}INP_3RhS_2$	$C_{25}H_{59}N_2P_4RhS_4$	$C_{48}H_{112}N_4P_8Rh_4S_8$	$C_{50.5}H_{118.50}IN_4P_8Rh_4S_8$
M_r	978.92	819.53	742.77	1661.30	1824.77
Crystal system	triclinic	triclinic	monoclinic	orthorhombic	monoclinic
Space group	$P\bar{1}$	$P\bar{1}$	$C2/c$	$Pnna$	$P2_1/n$
a [Å]	9.7307(4)	10.248(2)	17.3915(2)	17.7717(15)	21.2147(16)
b [Å]	10.8140(5)	12.404(3)	8.53700(10)	25.623(2)	15.1336(11)
c [Å]	22.8356(9)	14.575(3)	25.5604(3)	15.3352(13)	25.6461(19)
α [°]	94.269(4)	72.543(3)			
β [°]	94.247(3)	86.677(3)	109.7450(10)		103.8990(10)
γ [°]	104.391(4)	76.294(3)			
V [Å^3]	2310.40(17)	1716.9(7)	3571.86(7)	6983.0(10)	7992.7(10)
Z	2	2	4	4	4
$\rho_{calcd.}$ [g cm^{-1}]	1.407	1.585	1.381	1.580	1.516
T [K]	173(2)	173(2)	173(2)	100(2)	100(2)
F(000)	1026	828	1568	3424	3722
μ(Mo-K_α) [mm^{-1}]	1.54178	0.71073	1.54178	1.386	1.599
Total reflections	13022	18275	9062	31415	42661
Independent reflections	8396	7332	3369	5882	13857
R_{int}	0.0448	0.0300	0.0342	0.1003	0.0878
GoF	1.003	1.001	1.003	1.003	1.004
R_1, wR_2 [$I > 2\sigma(I)$]	0.0454, 0.1199	0.0446, 0.0995	0.0324, 0.0840	0.0422, 0.0735	0.0435, 0.0643
R_1, wR_2 (all data)	0.0535, 0.1252	0.0517, 0.1026	0.0341, 0.0852	0.0960, 0.0820	0.0967, 0.0700

Acknowledgments

The financial support from the Hong Kong Research Grants Council (project number 602310) and the Hong Kong University of Science and Technology is gratefully acknowledged.

[1] a) B. K. Burgess, D. J. Lowe, *Chem. Rev.* **1996**, *96*, 2983–3012; b) R. R. Eady, *Chem. Rev.* **1996**, *96*, 3013–3030; c) J. B. Howard, D. C. Rees, *Chem. Rev.* **1996**, *96*, 2965–2982; d) H. Beinert, R. H. Holm, E. Münck, *Science* **1997**, *277*, 653–659.
[2] E. I. Stiefel, K. Matsumoto (Eds.), *Transition Metal Sulfur Chemistry: Biological and Industrial Significance*, ACS Symposium Series 653, American Chemical Society, Washington, DC, **1996**, p. 101, and references cited therein.
[3] a) R. R. Chianelli, *Catal. Rev. Sci. Eng.* **1984**, *26*, 361–393; b) T. Kabe, A. Ishihara, W. Qian, *Hydrodesulfurization and Hydrodenitrogenation*, Wiley, Chichester, UK, **1999**.
[4] a) I. Haiduc, I. Silaghi-Dumitrescu, *Coord. Chem. Rev.* **1986**, *74*, 127–270; b) I. Haiduc, in: *Comprehensive Coordination Chemistry II* (Eds.: J. A. McCleverty, T. J. Meyer), Elsevier Pergamon, Amsterdam, **2004**, vol. 1, p. 323, and references cited therein.
[5] a) J. D. Woollins, *J. Chem. Soc., Dalton Trans.* **1996**, 2893–2901; b) T. Q. Ly, J. D. Woollins, *Coord. Chem. Rev.* **1998**, *176*, 451–481, and references cited therein; c) C. Silvestru, J. E. Drake, *Coord. Chem. Rev.* **2001**, *223*, 117–216; d) T. Chivers, J. S. Ritch, S. D. Robertson, J. Konn, H. M. Tuononen, *Acc. Chem. Res.* **2010**, *43*, 1053–1062.
[6] W.-M. Cheung, Q.-F. Zhang, I. D. Williams, W.-H. Leung, *Inorg. Chem.* **2007**, *46*, 5754–5762.
[7] a) W.-M. Cheung, W.-H. Chiu, X.-Y. Yi, Q.-F. Zhang, I. D. Williams, W.-H. Leung, *Organometallics* **2010**, *29*, 1981–1984; b) W.-H. Leung, K.-K. Lau, Q.-F. Zhang, W.-T. Wong, B.-Z. Tang, *Organometallics* **2000**, *19*, 2084–2089.
[8] Y. Misumi, H. Senio, Y. Mizobe, *J. Am. Chem. Soc.* **2009**, *131*, 14636–14637.
[9] L. M. Gilby, B. Piggott, *Polyhedron* **1999**, *18*, 1077–1082.
[10] D. Cupertino, R. Keyte, A. M. Z. Slawin, D. J. Williams, J. D. Woollins, *Inorg. Chem.* **1996**, *35*, 2695–2697.
[11] W.-M. Cheung, C.-Y. Lai, Q.-F. Zhang, W.-Y. Wong, I. D. Williams, W.-H. Leung, *Inorg. Chim. Acta* **2006**, *359*, 2712–2720.
[12] a) P. Bhattacharyya, A. M. Z. Slawin, M. B. Smith, *J. Chem. Soc., Dalton Trans.* **1998**, 2467–2475; b) J. Parr, M. B. Smith, A. M. Z. Slawin, *J. Organomet. Chem.* **1999**, *588*, 99–106; c) M. Valderrama, R. Contreras, M. P. Lamata, F. Viguri, D. Carmona, F. J. Lahoz, S. Elipe, L. A. Oro, *J. Organomet. Chem.* **2000**, *607*, 3–11.
[13] a) A. Gigoropoulos, D. Maganas, D. Symeonidis, P. Giastas, A. R. Cowley, P. Kyritsis, G. Pneumatikakis, *Eur. J. Inorg. Chem.* **2013**, 1170–1183; b) K. A. Chatziapostolou, K. A. Vallianatou, A. Grigoropoulos, C. P. Raptopoulou, A. Terzis, I. D. Kostas, P. Kyritsis, G. Pneumatikakis, *J. Organomet. Chem.* **2007**, *692*, 4129–4138.
[14] a) R. Ettorre, *Inorg. Nucl. Chem. Lett.* **1969**, *5*, 45; b) A. Yahav-Levi, I. Goldberg, A. Vigalok, *J. Am. Chem. Soc.* **2006**, *128*, 8710–8711.
[15] a) A. H. Roy, J. F. Hartwig, *J. Am. Chem. Soc.* **2001**, *123*, 1232–1233; b) A. H. Roy, J. F. Hartwig, *J. Am. Chem. Soc.* **2003**, *125*, 13944–13945.
[16] P. W. Vickers, J. M. Pearson, T. Ghaffar, H. Adams, A. Haynes, *J. Phys. Org. Chem.* **2004**, *17*, 1007–1016.
[17] a) C. M. Frech, D. Milstein, *J. Am. Chem. Soc.* **2006**, *128*, 12434–12435; b) M. Feller, A. M. Iron, L. J. W. Shimon, Y. Diskin-Posner, G. Leitus, D. Milstein, *J. Am. Chem. Soc.* **2008**, *130*, 14374–14375; c) M. Feller, P. Diskin-Posner, G. Leitus, L. J. W. Shimon, D. Milstein, *J. Am. Chem. Soc.* **2013**, *135*, 11040–11047.
[18] M. J. Bennett, P. B. Donaldson, *Inorg. Chem.* **1977**, *16*, 1581–1589.
[19] P. G. H. Troughton, A. C. Skapski, *Chem. Commun.* **1968**, 575–576.
[20] A. R. Siedle, R. A. Newmark, L. H. Pignolet, *Organometallics* **1984**, *3*, 855–859.
[21] A. M. Z. Slawin, M. B. Smith, J. D. Woollins, *J. Chem. Soc., Dalton Trans.* **1997**, 1877–1881.
[22] F. Cecconi, C. A. Ghilardi, S. Midollini, A. Orlandini, A. Vacca, J. A. Ramirez, *Inorg. Chim. Acta* **1989**, *155*, 5–6.
[23] D. Galli, L. Garlaschelli, G. Ciani, A. Fumagalli, S. Martinengo, A. Sironi, *J. Chem. Soc., Dalton Trans.* **1984**, 55–61.
[24] T. Iwasa, H. Shimada, A. Takami, H. Matsuzaka, Y. Ishii, M. Hidai, *Inorg. Chem.* **1999**, *38*, 2851–2859.
[25] N. Zúñiga-Villarreal, M. Reyes-Lezama, G. Espinosa, *J. Organomet. Chem.* **2001**, *626*, 113–117.
[26] T. G. Schenck, C. R. C. Milne, J. F. Sawyer, B. Bosnich, *Inorg. Chem.* **1985**, *24*, 2338–2344.
[27] D. Cupertino, R. Keyte, A. M. Z. Slawin, D. J. Williams, J. D. Woollins, *Inorg. Chem.* **1996**, *35*, 2695–2697.
[28] J. A. Osborn, G. Wilkinson, *Inorg. Synth.* **1967**, *10*, 67.
[29] A. van der Ent, A. L. Onderdelinden, *Inorg. Synth.* **1990**, *28*, 90.
[30] a) Bruker, *SADABS*, Bruker AXS Inc., Madison, Wisconsin, USA, **2001**.
[31] Oxford Diffraction, *CrysAlis RED*, version 1.171.33.2, Oxford Diffraction Ltd, Abingdon, England, **2006**.
[32] G. M. Sheldrick, *Acta Crystallogr., Sect. A* **2008**, *64*, 112–122.

Received: February 19, 2014
Published Online: May 22, 2014

